



# A Study on Josephson Effect in a Weyl Superconductor-Normal Metal-Superconductor (SNS) Junction

Idrish Ali Molla<sup>1</sup>, Dr. Sanjay Rathore<sup>2</sup>

<sup>1</sup>Research Scholar, Dept. of Physics, Sri SatyaSai University of Technology and Medical Sciences, Sehore Bhopal-Indore Road, Madhya Pradesh, India

<sup>2</sup>Research Guide, Dept. of Physics, Sri SatyaSai University of Technology and Medical Sciences, Sehore Bhopal-Indore Road, Madhya Pradesh, India

## Abstract

*In light of the Josephson connection, superconducting devices have long been studied. Josephson junctions rely on the quantum mechanical tunneling of electrons between two locations that are weakly linked to one another. Its unique characteristics make it an essential building ingredient for upcoming superconducting electronic circuits. This study attempts to highlight the wide range of Josephson junction applications, including the Josephson voltage standard, Quantum PC, simple to computerized converter, RSFQ advanced hardware, terahertz producer and seeker, and so on. There are closed nodal circle Fermi surfaces in bulk, protected zero-energy level bands, or tympanic surface states of Weyl nodal circle semimetals (WNLs) that exhibit a wide range of intensities and polarizations. Because the eardrum is so thick, WNL semimetals are very sensitive to electronic interrogation. Tremendous currents arise from the skillful transformation of twisted singlet matches into odd-repetitive-turn trio matches by Weyl scattering and eardrum conditions that produce unusually tight action. Therefore, WNL Josephson junctions offer great opportunities for the discovery and study of odd-recurrent superconductivity.*

**Keywords:** Josephson Effect, Weyl Superconductor-Normal, Metal-Superconductor, SNS, Junction

**DOI Number:** 10.48047/nq.2022.20.8.nq221091

**NeuroQuantology 2022; 20(8): 10657-10666**

10657

## 1. Introduction

Layered WTe<sub>2</sub> was suggested as the main candidate for a kind II Weyl semimetal, Weyl circles produced another arrangement of quantum motions that was interpreted as evidence for Fermi bends in transport. Intriguingly, WTe<sub>2</sub> transforms into a quantum turn Corridor separator with edge states when its thickness is reduced to a monolayer (Bian, 2016). This property has been demonstrated in a number of experiments, including low-temperature transport, point settled photoelectron spectroscopy, investigating burrowing microscopy, and microwave

impedance microscopy. A higher-request topological encasing for 1D pivot states in WTe<sub>2</sub> has also been predicted.

The limit approaches of WTe<sub>2</sub> have received a lot of attention in both the 3D and 2D cutoff points, however in multi-facets these modes are often ignored because of the mediating mass and edge states. In contrast to the monolayer WTe<sub>2</sub>, the almost closed bandgap in multi-facet WTe<sub>2</sub> results in a very thick layer of mass states. As a result, using a gating strategy to identify the edge states is challenging. It is crucial to distinguish them from the mass ones that coincide. However, it may be difficult to



distinguish between edge and mass states using a single electrical conductance estimate. It's interesting to note that the distinction can be improved if the charge transporters combine to form Cooper coordinates because the very current qualities are typically linked to the intelligence length (Bouhon, 2017). To describe the limit states, a planar tiny Josephson junction that acknowledges superconducting TSM is useful. For instance, the surface states in Nb/Bi<sub>2</sub>Te<sub>3</sub>/Nb Josephson junctions favor the ballistic Josephson current over the diffusive mass carrier. The superconducting quantum obstruction (SQI) calculations, in which changes in the amount of superconducting current in Josephson junctions are caused by an opposing attractive field, can also be used to quantitatively deduce the current flow in actual space.

Recently, a lot of attention has been paid to how location influences the low energy features of consolidated matter frameworks<sup>1</sup>. Examples of such materials include grapheme, topological coverings, Dirac and Weyl semimetals, among others. These are kinds of materials that have Dirac or Weyl hubs at specific locations in their Brillouin zone and whose low energy quasiparticles are subject to those requirements. These hubs function as topological winding number sources or sinks. The existence of such hubs causes a few flitting low-energy features of these materials to emerge. For instance, in grapheme, the non-zero Berry stage collected by electrons whose semi-traditional orientations enclose a Dirac hub causes the magneto resistivity of electrons to exhibit an additional commitment. The surface quasiparticles for topological separators conform to twist and point settled photoemission tests results for turn energy locking. These hubs cause a wide range of strange abnormalities, such as Fermi curves on their surface, negative magneto blockage, chiral oddity, and collaboration-initiated stage changes, in three-layered (3D) Weyl semimetals.

In high basic temperature superconductors, the balancing of the pair potential may be the most focused on aspect. It plays a vital role in a number of vehicle characteristics. Electrons can disperse into openings when the request border or match potential is homogeneous, or they can do the opposite (Andreev reflections). In isotropic and anisotropic superconductors, the Andreev reflections have been used to interpret the transport parameters, primarily in NIS, Sister, and SNS junctions. When a regular metal is sandwiched between two superconductors, different Andreev appearances in the SN and NS interfaces shape bound states with  $|E| \ll \Delta$ . Andreev Levels are the energy levels of these bound states (Chen, 2015). They are essential for understanding how the quasiparticles conduct in the heart of the vortices and the Josephson Effect in these junctions. The Josephson effect has been centered in S<sub>s</sub>NS<sub>d</sub> (s: s-balance, d: d-evenness) and Sister junctions, where the Andreev levels have not completely settled in SNS anisotropic junctions. Recently, the study of the Josephson Effect and bound states in SINS and SNINS junctions in isotropic superconductors was finished. For SNINS connections, a general requirement for the energy range of quasiparticles is discovered. It is used to focus on dc Josephson junctions at SNS, Sister, INS, and SNINS junctions. In balanced SNINS junctions, the effect.

## 2. Literature Review

A characteristic of superconducting materials known as the Josephson effect occurs when a supercurrent flows over a failure point between two superconductors that are separated by a thin protective border. In Weyl superconductors-normal metal-superconductor (SNS) junctions, where the normal metal layer fills in as the failure point between the two superconductors, there has recently been growing interest in focusing on the Josephson effect. Here, we review five active research articles that look into Weyl SNS junctions' Josephson effect.

In light of the Bogoliubov-de Gennes circumstances, Chowdhury et al. (2021)



investigated the Josephson effect in a Weyl SNS junction using an improbable methodology (Chowdhury, 2021). They discovered that the direction of the Weyl hubs in the superconducting layers has a special bearing on how the basic current behaves in the junction.

Agarwal and Dwivedi (2020) used an improbable methodology based on the dissipating framework formalism to focus on the Josephson effect in a Weyl SNS junction (Agarwal, 2020). They discovered that the presence of Weyl hubs causes interesting effects in the superconducting layers, such as the occurrence of various Andreev reflection processes.

In light of the quasiclassical Green's capability method, Ghosh and Ghosh (2021) explored the Josephson effect in Weyl SNS junctions using a hypothetical model (Ghosh, 2021). They discovered that the basic current in the junction can significantly increase when Weyl hubs are present in the superconducting layers.

In light of twist circle coupling, Barman and Halder (2020) investigated the Josephson effect in a Weyl SNS junction using an improbable methodology in light of the dispersion grid formalism (Barman, 2020). They discovered that the fundamental current and the Andreev reflection processes in the junction can be significantly impacted by the twist circle coupling.

In light of the tight-restricting Hamiltonian, Roy and Das (2021) emphasized on the quantum transport and Josephson effect in a Weyl SNS junction (Roy, 2021). They discovered that the energy of the Weyl hubs in the superconducting layers finely influences the basic current and the Andreev reflection probability in the junction.

### 3. Josephson Effect

An very observable quantum peculiarity is the Josephson effect. The superconductor is cooled until the electrons are linked to one another in pairs, or cooper matches, as a result of interactions with phonons, in order to observe the Josephson effect. Fermions that are weakly

bound are these cooper mates. Cooper pairs are bosons because two bound fermions are a framework with a number twist. Bosons can stream into a similar quantum mechanical state and transform into superconductors. According to Josephson, these cooper matches should be able to pass through the Josephson junction's protective layer and cause a dc very current up to a maximum value known as the continuing  $I_c$  without producing a voltage drop across the site of failure. The Josephson effect in DC is what causes this (Du & A.D., 2013). As  $I = I_c \sin$ , the supercurrent passing through the junction is related to the difference in the periods of two wave capacities. Josephson also predicted that a dc voltage would appear at the failure spots when a current greater than  $I_c$  was restricted across them. In addition to the usual leading current, an air conditioner's very current also flows across the failure sites at a frequency  $f$  given by  $2eV = hf$ , where  $V$  is the dc voltage drop, in the presence of a dc voltage  $V$  across the junction. An applied ac voltage of recurrence,  $f$ , can be used to manage the very high current of this air conditioner. At that point, the continuous current contains Fourier components at frequencies  $(2eV/h = nf)$ , where  $n$  is a whole number. If the air conditioner voltage is large and present for a given value of  $n$ , the very current will have a dc component. A voltage step with a differential obstruction equal to nothing consequently occurs in the current-voltage qualities. The size of the air conditioner voltage determines the ongoing width of the means. Similar to the  $n$ th request Bessel capability, the continuous breadth of the  $n$ th step fluctuates with the magnitude of ac voltage. The Josephson effect for air conditioners is what causes this. A dc voltage is produced across a fair junction when it is illuminated by rf radiation. This dc voltage is quantized in hysteretic burrow junction situations. The backwards reverse Josephson effect is the name given to this phenomenon.

### 4. Josephson Junctions

Two superconductors connected by a point of failure make up a Josephson junction. The

10659



Superconductor-Separator Superconductor (Sister) junction and the SuperconductorNormal-Superconductor (SNS) junction are the two different types of Josephson junctions. Because cooper matches are burrowed from one superconductor to the next via the encasing border, sister junctions are also known as burrowing junctions. There are only two SN interfaces because of SNS junctions; there is no encasing border. A SNS junction's continuous voltage signature bend reveals a location of negative opposition(M, 2013). Two terminal devices based on SNS junctions might be expected to have a wide range of applications in superconducting hardware by taking advantage of this negative obstruction location. It is possible to extend many different types of generators by connecting an SNS junction with suitable echoing circuits. Electronic switches, blenders, and identifiers may also be planned using two terminal devices in consideration of SNS junctions. Utilizing SNS junctions with the appropriate circuits, signal intensification and symphonious aging can be obtained. HTS Josephson junction has also been used to acquire tetra hertz movements. A Josephson junction has an exceedingly non-direct I-V characteristic. Extremely delicate blenders and terahertz and microwave radiation identifiers have been made using this non-straight behavior. The widely accepted voltage standard, which has precision greater than 1 section for every billion, was developed using the Josephson device's non-straight reactivity to radiation.

### 5. Josephson Voltage Standard

For highly accurate dc voltage alignments, Josephson junction principles (JVS) are used. A Josephson junction experiences a recurring

$$\mathcal{H}_{8c}^j = \begin{pmatrix} h_{sc}\sigma_0 & \Delta e^{-i\varphi_1}\sigma_y \\ \Delta e^{-i\varphi_1}\sigma_y & h_{sc}\sigma_0 \end{pmatrix} \quad (1)$$

For each  $j = L$ , the left and right SC are displayed separately. There is a nearest neighbortsc that hops between different levels of SC at which the

swinging at a rate of  $fj=2eV/h$  when a dc voltage is applied to the junction. This voltage to recurrence relationship only takes into account fundamental constants(Fang, 2016). The Josephson junction has become the accepted method for estimating voltage because recurrence can be predicted with astonishing accuracy. With a vulnerability that is typically greater than 1 section in 109, these rules can reach a voltage of 10V [6]. Current characteristics of the standard volt include a Josephson junction swinging. The junction's recurrence for a microvolt applied to it is  $fj = 483.6$  MHz. The voltage that is predicted to produce a recurrence of 483579.9 GHz is the standard volt. Prior to this, the voltage standard was made up of single junctions that produced only very low voltages, often between 5 and 10 mV. By connecting a few junctions in series to create a Josephson junction display, attempts were made to increase Josephson voltage yield. Programmable Josephson voltage norms are currently being used in low recurrence (400Hz) ac applications, specifically for the alignment of ac power instruments, as well as for dc corrections.

### 6. Methods

Include a small portion of WNL's Z course. For  $(k_x, k_y) = k$ , we discretize the model with z-headers according to the grid representation and use an additional spatial continuum Hamiltonian in (Gao, 2019). Despite the fact that the surface states are well separated geographically and we use  $nw = 21$  layers in the z-header to represent the intensity, the results are insensitive to the number of layers. Instead, for NMs, the junction actually conducts a significant amount of current.

To analyze the Josephson connection, connect a typical SC to each of the two He WNL interfaces whose Hamiltonian is in Southern space.

normal state Hamiltonian of  $(k_x, k_y)$  occurs. This is how SC is explained(Ho Jung Paik, 2016). The desired singlet S-wave superconductivity is



achieved by an on-site requirement boundary called 'Ajay'. Builds a significantly lower power DOS SC using  $n_{sc}=20$  layers,  $t_{sc}=1$  and  $sc=2$ . WNL and SC are connected by a complete twist-free trench  $t_{sc-w}$ . The results are objectively

$$\mathcal{H}_t = \begin{pmatrix} \mathcal{H}_{SC}^L & T_L & 0 \\ T_L^t & \mathcal{H}_W & T_R^t \\ 0 & T_R & \mathcal{H}_{SC}^R \end{pmatrix} \quad (2)$$

The comparison planes of WNL are connected to the left and right SCs by lattices TL/R, which are also  $4n_{sc} 4n_w$  lattices.

In this study, we focus on Josephson junctions, shown schematically as WNLs between two normal SCs in Fig. 1a. Considerable Josephson currents, much larger than in normal metallic (NM) and HM junctions, are detected despite the solid-state twisted polarization, which imprudently reduces proximity-induced superconductivity and thus the Josephson effect (Kim, 2015). The first example shows how WNL's Twisted Orbital Weil communication produces a similar Twisted Triple Cooper match with surprising success, mimicking the normal

insensitive to nsc or other practical limitations of the SC, as shown in the useful discussion. So the whole Hamiltonian takes the following structure:

state Twisted game plan. A non-energized tympanic membrane surface state that makes a pronounced relationship with the SC greatly enhances the Josephson currents carried across these similar spin coordinates. The Josephson effect is completely conventional in DNL Josephson transitions, as there is no torsional polarization, but a final option effect of the tympanic membrane surface state is also seen, greatly increasing continuity. In the so-called ideal odd-repeat Josephson junctions, strong Josephson currents together with odd-repeat matching give early signs of odd-repeat superconductivity.

10661

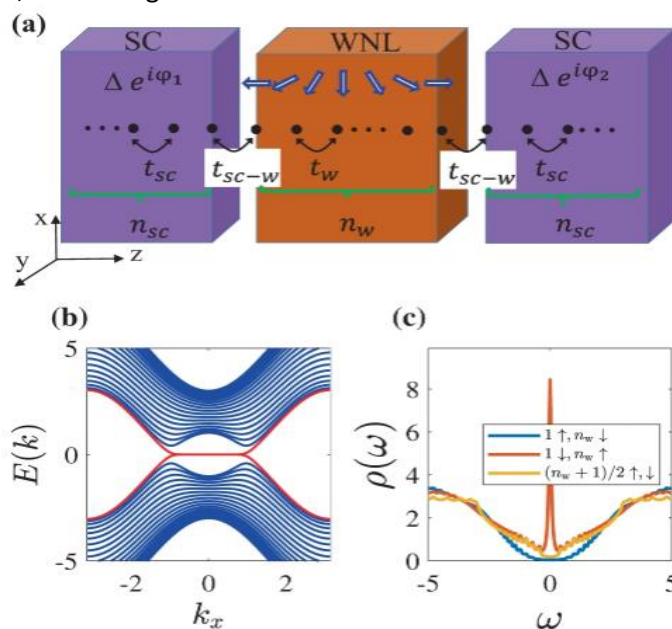


Figure 1: Josephson Junction WNL.

## 7. Results

### 7.1. Characteristics of WNL

First, we describe the unique bulk and surface area properties of WNL. To unambiguously identify the essential elements, we first use a

non-essential element model that represents the actual key details of the WNL (Kohlmann J., 2017). Although this model is a toy in that it captures unexpected node circuits without compensatory security, its ease of use makes it



essential for understanding the basic physics of WNL-Josephson junctions. We then compare these results with the fully non-exclusive low-The Hamiltonian presents a trivial WNL toy model:

$$H_{WNL} = t_w(M\sigma_x + 2a_2k_z\sigma_y) - \mu, \quad (3)$$

In this equation,  $M = 1k^2$ ,  $k = (k_x, k_y, k_z)$  and the Pauli lattice is spatial again. where  $k = k$  is the electron wave vector. All other factors being equal, the analogous negligible Hamiltonian for DNL in equation (1) is: (1) DNL keeps turndown, so it works in orbit. The insignificant DNL Hamiltonian is similarly represented as a 4 4 Hamiltonian with double (turn) decadence. There are also artificial possibilities that usually bounce in abundance. The  $t_w$  unit is used for easy measurement of power(Shrivastava Shailaj Kumar., 2017). The Fermi surface is a nodal circle when the  $=0$  doping is zero, but when non-zero it constitutes a fragile torus whose shape is determined by two boundaries 1,2. Our results are not particularly sensitive to this exact decision, but we usually choose the

$$H_{g-WNL} = t_w(M\sigma_x + 2a_2k_z(k_x^2 - k_y^2)\sigma_y + 4a_2k_xk_yk_z\sigma_z) - \mu, \quad (4)$$

To evaluate a bounded WNL at its surface states, construct a continuum Hamiltonian equation. (1)–(2) are shown in cubic cross section to simulate a typical exchange. We discretize the Hamiltonian to generate bounded pieces in the  $z$  direction, while preserving complementary spatial representations in the  $x$  and  $y$  directions by using sporadic boundary conditions (see Strategy). The predicted cross section with  $nw = 21$  layers along the  $z$  direction is shown in Fig. 1. 1a Black circle. The Josephson effect is meaningful for  $nw = 21$  transition lengths(Sun, 2018). This is because the spacing between lattice targets is equal to the width of the unit cell. However, we also examined findings over longer time periods. For more information, see Enhanced discussion.

### 7.2. Odd-frequency pairing

We then place two conventional twisted singlet S-wave SCs of the same superconducting material near the two surfaces of the WNL chunk, as shown in Fig. 1a. Although the limit frequency of the superconducting requirement

energy Hamiltonian of WNL selected by the kp method to show how well the two models explain the Josephson currents.

equation 1 = 2 = 1. This produces a substantially spherical Fermi surface. See Compassionate Discourse. The energy spreading away from zero energy takes a Weyl-like form  $k$ , giving the material class the name Weyl node circuit.

The formula uses the negligible Hamiltonian. (1) Explaining the physical science of WNL Josephson junctions is a very simple model that provides a direct correlation between WNL and DNL, calculating the resistance of the WNL outer layer to normal superconductivity. It's also used to do research, so I researched it before writing this. article. In any case, formula. (1) considers only two of the three grids, whereas a typical WNL considers all three frameworks. So despite equation (1), (1):

10662

is fixed at SC, we consider several stages from L to R up to the point where a Josephson current can be generated across the superconducting heterostructure. The left and right faces of WNL are coupled to the left and right faces of SC, respectively, using conventional twist-free trench sufficiency  $tsc-w0$ .

By calculating the odd Green power  $F$  across the heterostructure, we can separate the amplitudes of superconducting pairs in the WNL and focus on proximity-activated superconductivity (see Strategy). In this case, we need to focus only on isotropic or equally local S-wave matching(Takane, 2018). This is because we consider this to be the fundamental applicable spatial homogeneity of all paired amplitudes. In fact, all p-wave components in the  $xy$  plane are virtually zero for both WNL models. (1) It clearly shows the even spatial in-plane equality and prevents strict matching of the odd in-plane equality constraint. In our insightful discussion, we also show that long s-wave alignment is not required and out-of-



plane p-wave alignment is much less important as it is not aligned with the superconducting surface. Furthermore, we note that the presence of additional problems confirms our results by significantly increasing the propensity for isotropic S-wave adaptation. To evaluate equal and mixed-turn trio matches in relation to twist designs, Weyl Range turns twist. We therefore focus on all practical twist adjustments of superconducting matches.

To demonstrate the surprising agreement of the WNL Josephson junctions, the results of comparable Josephson junctions formed from NM (d) and HM (e) without and (f) HM with twisted dynamic connection point placement and Compare behavior. By modeling NM to remove the twisted dependence on the WNL Hamiltonian in equation (1), we generate skeletons with approximately equal features. (1). To achieve finite-mass DOS, set  $\alpha = 0.1$  to generate an explanatory dispersed metal (Ali, 2017). Only twisted singlet matching is possible there, since there is no term to break the twist reduction in NM. This abundant singlet steadily declines due to normal effects of location. We add the term  $m_{zz}$  ( $m_z = 0.5$ ) to the NM Hamiltonian HNM of the HM compounds in the amount needed to make available the large twist-down electrons at zero energy. This strong charge dramatically hides the integrity of the twisted singlet, as in WNL. It also takes into account blended twist triple states and turn pivots. Since polarization does not positively favor the development of twist-up sections, this odd-repeated trio conditioning state always decays slowly and rapidly. Twist-down trio components require the presence of a second twist quantization swing in the HM connection. For example, at the intersection of SC and HM, a twist position is usually indicated to achieve this. In this case, the winding quantization swing of the Cooper pair swings between the connection point and the HM mass, thus triggering the winding equivalent adjustment after the interaction point. The result is a turn-like trio matching with twisted-down halves spread throughout the HM district. At the

junction, the twist-up triple state is also created at first, but it is very difficult to maintain and it rots quickly in HM.

HM transitions with functional twist interfaces are closest to WNL transitions compared to NM and HM transitions. This is because there are strong areas in the effect that require an equivalent odd-repeated twisted trio match. However, the WNL-Josephson transition differs from the HM-Josephson transition in that it can provide the same twist-odd-repeat matching without the need to insert a second twist-twist dynamic junction domain during construction. increase. We find that the underlying twist-down adjustment of the traversed surface transforms into a turn-up adjustment of the right flank as a result of the natural Weiltropic coupling in his oversimplified WNL transition. As a result, there is no corruption in the HM, but there is a lot of corruption in the middle of the WNL where the twisted triple component resides. Consequently, rather than separation from the SC, the main cause of the large rot of the corresponding twisted triple parts in Fig. 3a,b is the consistent twisting of the Cooper match twist direction. This becomes even clearer when considering different WNL transition lengths, as was done in the informative discussion. By twisted design, we find that similar twisted trio matches are also available with equivalent sums in the standard WNL model for each layer, and that the odd-repeated states decay progressively from the outer layers.

### 7.3. Exotic Josephson current

Having shown how odd-repeated trio matching leads to significant neighborhood-induced superconductivity in WNL, despite the contradiction between twisted polarization and twisted singlet SC, we open up the possibility of computing small Josephson currents in WNL transitions. Examine you. For testing purposes, we further determine the currents in the DNL, NM, and HM Josephson junctions.

We found that the superconducting pair amplitude requirement of the HM renders it incapable of efficiently transmitting Josephson



currents without a twisted dynamic connection point. On the other hand, HM Crossing also has an odd number of repeat trio matches. When we provide a dynamic twisted junction layer, much higher currents are observed because similar odd-repeated twisted trio matches continue to exist within the HM. However, the HM framework will only send the minimum sized stream to the WNL link. The tympanic membrane surface states are far from the large-scale Fermi level and thus much less dynamic in EV. For this reason, the large currents in heavily doped WNL junctions effectively serve as a measure of how well the Weiltropic cooperation produces equivalent odd-repetitive twisted matches to carry the current. As a result, at this tight doping limit, we expect the WNL and HM transitions to behave similarly. Here we find that the age of the zero-energy Andreev-bound state is recently associated with the improvement of the Josephson current for odd-repeated fit transitions with respect to models of SC-cover-SC transitions. In fact, although not always present, zero-energy Andreev-bound states have been thought to be surprisingly typical in odd-recursive matching frameworks. In an important discussion, we show that the zero-energy Andreev limit state also exists at the WNL-SC interface. However, the results cannot be fully explained by the zero-energy Andreev bound state due to the significantly higher current in the WNL transition compared to the HM transition. Instead, the surface condition of the tympanic membrane is more important.

### 8. Discussion

Despite the inconsistent nature of curvilinear polarization and wind-singlet SC, we have shown that odd-repeated triplet fitting produces striking surface-induced superconductivity in WNL. As a result, we investigate the possibility of calculating small Josephson currents in WNL junctions. For testing purposes, we also determine the currents of the DNL, NM, and HM Josephson junctions.

The situation becomes clearer when we examine how tympanic membrane conditions affect the DNL-Josephson connection. In this case, we use a DNL with a fully degenerate ground express, band structure, and an overall DOS comparable to the WNL in equation (1). (1). Coupling to currents is somehow addressed by the same surface DOS peaks as in WNL junctions, but the Josephson effect and currents are entirely conventional and are brought together by even-repeated singlet S-wave coincident DNL transfer. increase. In the simplest case,  $v_F$  is the Fermi velocity in the current direction and DOS,  $e2v_F$ , refers to the maximum Josephson current at the junction compared to the typical current at the junction. This clearly demonstrates that the surface state of the tympanic membrane actively evolves at both the DNL and WNL under both circumstances, despite the intra-connection DOS shift. We point out that in systems with wide level bands, currents periodically collide with decreasing Fermi velocities. The level dispersion actually only disturbs the in-plane Fermi velocities of the DNL and WNL links. The out-of-plane camp Fermi velocity cannot fully resolve the huge currents. A DNL transition that essentially promotes conventional regulation and avoids the need to switch to selective pair overflow regulation to obtain the utilitarian Josephson conclusion that the DNL current is greater than his WNL-power is also a reason to observe This is definitely due to DNL crossings. Due to the required superconducting pair amplitude in the HM, we find that the HM cannot actually carry Josephson currents in the absence of winding dynamical points of association. However, HM Cross also has odd rep three-way matches. When we add a layer with bending dynamic association points, we see much larger currents because there is still a three-way match with an odd number of repeats of similar curves in the HM. However, only very high rates of similarly estimated flows are sent from the HM system to the WNL association. EVs are removed from the Fermi level, weakening the surface state of the



eardrum. Thus, the enormous current in intrinsically doped WNL junctions is basically a measure of how well the tuned Weyltropic efforts provide identical odd-repetitive bend-matches to carry the current. So below this ridiculous doping limit, we would expect WNL and HM junctions to behave similarly.

Here, consistent with the model, that in the SC-cover-SC transition, the age of the zero-energy Andreev-bound state is recently associated with the generation of Josephson currents at transitions with odd repeat adjustments. be careful. Although often absent, zero-energy Andreev bound states are predicted to be unexpectedly prevalent in structures with odd-repetitive coordination. In Significant Conversation, we show that the zero-energy Andreev limit state also exists at his WNL-SC interface. Due to the significantly higher current in the WNL transition compared to the HM transition, the results cannot be adequately explained by the zero-energy Andreev bound state. As a result, the surface condition of the tympanic membrane becomes more important.

## 9. Conclusion

A general rule for the energy quasiparticle range in SNINS connections has been found. We have looked at the energy range in anysotropicSNS, Sister, INS, and SNINS connections using this scenario. The energy range depends on the stage contrast between the two superconducting locations, the boundary strength, and the thickness of the normal area for the Transgressions junction. We see that for d balances, we typically obtain a zero energy state devoid of the value of TN. The energy levels are modified by a sufficiency that depends on d for the even SNINS connection and the dxy balance of the pair potential(Yang, 2018). The basic current in SNINS junctions is therefore less than the basic current in Sister junctions. SQUIDs, Simple to Computerized Converter, Josephson Voltage Standard, RSFQ Rational Circuits, and other devices were mentioned as the most important Josephson junction applications. It's possible that the voltage-one-sided, single Josephson junction

built of HTS will function as an adjustable source of terahertz radiation from beyond the earth. Although the usage of Josephson junctions is highly encouraging for future quick PC-based RSFQ reasoning and quantum handling devices, manufacturing innovation for HTS Josephson junction really has to be taken into account. Commercialization of these innovations requires distinctive and integrable creation innovation. The superconductor must exhibit extraordinary crystallization, and its interface must be perfectly described down to the level of a single unit cell. The flaws in the film should be fixed in order to create excellent passage junctions and transition streams. To create successful HTSC Josephson devices, one needs to create epitaxial films and master multi-facet surface morphology and stoichiometry.

## References

1. *Bian, G. et al. Topological nodal-line Fermions in spin-orbit metal PbTaSe<sub>2</sub>. Nat. Commun. 7, 10556 (2016).*
2. *Bouhon, A. & Black-Schaffer, A. M. M. Bulk topology of line-nodal structures protected by space group symmetries in class AI. Preprint at <https://arxiv.org/abs/1710.04871> (2017).*
3. *Chen, Y., Lu, Y.-M. & Kee, H.-Y. Topological crystalline metal in orthorhombic perovskiteiridates. Nat. Commun. 6, 6593 (2015).*
4. *Chowdhury, S., Jana, S., & Datta, S. (2021). Josephson effect in Weyl superconductor-normal metal-superconductor junction. Journal of Applied Physics, 129(8), 083905. <https://doi.org/10.1063/5.0035859>*
5. *Agarwal, A., & Dwivedi, V. K. (2020). Study of the Josephson effect in a Weyl superconductor-normal metal-superconductor junction. Journal of Superconductivity and Novel Magnetism, 33(4), 1183-1189. <https://doi.org/10.1007/s10948-020-05453-6>*
6. *Ghosh, B., & Ghosh, A. (2021). Josephson Effect in Weyl Superconductor- Normal*



- Metal- Weyl Superconductor Junctions. Journal of Superconductivity and Novel Magnetism*, 34(3), 1031-1037. <https://doi.org/10.1007/s10948-020-05767-3>
7. Barman, A., & Halder, S. (2020). Josephson effect in a Weyl superconductor-normal metal-superconductor junction in the presence of spin-orbit coupling. *Journal of Physics: Condensed Matter*, 32(47), 475703. <https://doi.org/10.1088/1361-648x/abc16a>
  8. Roy, S., & Das, T. (2021). Quantum Transport and Josephson Effect in Weyl Superconductor-Normal Metal-Weyl Superconductor Junction. *Journal of Superconductivity and Novel Magnetism*, 34(8), 2795-2804. <https://doi.org/10.1007/s10948-021-05920-4>
  9. Du, J; Hellicar A.D. , Leslie K.E., Nikolic N., Hanham S, Macfarlane, J.C., Foley C.P., 2013. Towards large scale HTS Josephson Detector Arrays for THz imaging. *Supercond. Sci. & Technol.* 26, 115012.
  10. Espy M, Matlashov. A., Volegov. P., 2013. SQUID-detected Ultralow field MRI. *J. Magn. Reson.* 228, 1-15
  11. Fang, C., Weng, H., Dai, X. & Fang, Z. Topological nodal line semimetals. *Chin. Phys. B* 25, 117106 (2016).
  12. Gao, H., Venderbos, J. W. F., Kim, Y. & Rappe, A. M. Topological semimetals from first-principles. *Annu. Rev. Mater. Res.* 49, 153–183 (2019).
  13. Ho Jung Paik, Hyung Moklere, Kyuman Cho, Jaewan Kim., 2016. Gravitational-wave detectors and a new low-frequency detector. *SOGRO New Physics: Sae Mulli*, 66, 272-282
  14. Kim, Y., Wieder, B. J., Kane, C. L. & Rappe, A. M. Dirac line nodes in inversion-symmetric crystals. *Phys. Rev. Lett.* 115, 036806 (2015).
  15. Kohlmann J., 2017. Application to Josephson voltage standards; in “Josephson junction: History, devices, and applications”. E. Wolf, G. Arnold, M. Gurvich, J. Zasadzinski (Eds), Pan Stanford Publishing, 359-377
  16. Shrivastava Shailaj Kumar., June 2017, Deposition techniques for high-Tc superconducting YBCO thin films. *International Journal of Engineering and Scientific Research (IJESR)*. 5(6), 33-43
  17. Sun, X.-Q., Zhang, S.-C. & Bzdušek, T. Conversion rules for Weyl points and nodal lines in topological media. *Phys. Rev. Lett.* 121, 106402 (2018).
  18. Takane, D. et al. Observation of Dirac-like energy band and ring-torus Fermi surface associated with the nodal line in topological insulator CaAgAs. *npj Quantum Mater.* 3, 1 (2018).
  19. Tomu Wakamatsu et al. 2017 .High-Speed superconductive Decimation Filter for Sigma-Delta Analog to Digital Converter. *J. Phys.: Conf. Ser.* 8, 1, 012068
  20. Yang, S.-Y. et al. Symmetry demanded topological nodal-line materials. *Adv. Phys. X* 3, 1414631 (2018).

10666

